

Proposal of Impedance Control for Electric Vehicles with Wheel Resolver - Application to Hand Assisted Parking and Position Adjustment -

T. Enmei*, H.Fujimoto**, Y. Hori***

The University of Tokyo

5-1-5, Kashiwanoha, Kashiwa, Chiba, 277-8561 Japan

Phone: +81-4-7136-3881

Email: enmei14@hflab.k.u-tokyo.ac.jp*, fujimoto@hflab.k.u-tokyo.ac.jp**, hori@hflab.k.u-tokyo.ac.jp***

Abstract—Electric vehicles (EVs) have an advantage over internal combustion vehicles in that the forces applied to the wheel can be estimated from the wheel velocity and input torque. By exploiting this feature, the authors propose to apply force control, which is often used for industrial robots, to EVs in order to achieve much more human friendly EVs. Many applications of force control for EVs are possible. In this paper, the hand parking assist control is proposed. The position of the vehicle body is adjusted by the human hand outside vehicles. The high backdrivability is achieved by using impedance control and driving force control. External forces applied by human hands and driving forces are estimated by disturbance observer (DOB). Some assist control methods are proposed and the most appropriate one is discussed with simulations by considering road surface change and resolution of wheel resolver. Finally, the effectiveness of the proposed method is demonstrated by an experiment.

I. INTRODUCTION

As the concerns of environmental problems increases, Electric Vehicles (EVs) are getting attention. EVs are superior to internal combustion vehicles not only in the environmental aspect but also in controllability[1]. The response of electric motors is much faster than fuel engine, the driving force on wheels can be estimated[2], and it is possible to distribute driving force within each of the four EV motors.

There are many traction control methods based on these advantages[3]. Our research group also proposed many EV control methods such as slip ratio estimation[4] and direct driving force control method[2].

In this research, force control for EV is proposed. It is based on EVs' ability to estimate external force, thus realizing backdrivable EVs. Researches on force control are popular in industrial fields so that people and robots can collaborate[5], [6]. By applying force control to EV, vehicles become more human friendly. The proposed method is realized by the use of driving force control and impedance control.

There can be many applications of force control for EVs. In this paper we propose hand assisted parking. Many people are not good at parking because position adjustment work is very different from usual driving. This lack of driving skill sometimes leads to serious accidents.



Fig. 1. Experimental setup: FPEV2-Kanon.

By applying force control to EVs, it became possible to adjust vehicle position by human hand. There have been many researches about parking methods such as automatic-parking[7]. Hand assisted parking is one of the most instinctive method for humans. The proposed method is convenient in cases which automatic parking cannot cope with. Moreover, impact force in case of collision can be reduced with the aid of impedance control[8].

In section II, experimental vehicle models and its control methods are introduced. In section III, some assistance methods are discussed. By simulations and experiments, control performance of the proposals are verified in section IV and section V. Finally, the conclusion remarks are in section VI.

II. MODELING OF EV AND CONTROL METHODS

The experimental setup and its physical model are shown in this section. Then, driving force control (DFC) and impedance control are introduced.

A. Experimental device

Fig. 1 shows the experimental setup and the concept of this research. The vehicle used in this study is FPEV2-Kanon, manufactured by authors' research group. Kanon has four outer-rotor type in-wheel motors and each wheel can be independently controlled. The specifications of the vehicle are

TABLE I
VEHICLE SPECIFICATION.

Vehicle mass M	854 kg
Wheelbase l	1.72 m
Distance from center gravity to front axle l_f	1.01 m
Distance from center gravity to rear axle l_r	0.702 m
Gravity height h_g	0.51 m
Front wheel inertia J_{ω_f}	$1.24 \text{ kg} \cdot \text{m}^2$
Rear wheel inertia J_{ω_r}	$1.26 \text{ kg} \cdot \text{m}^2$
Wheel radius r	0.302 m

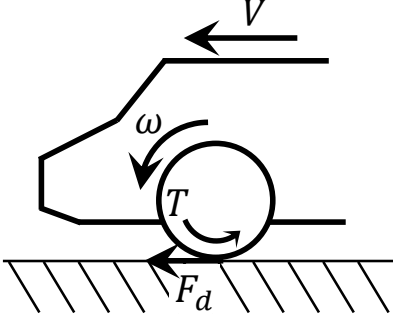


Fig. 2. Physical model of Electric Vehicle.

shown on Table I. In this research, rear wheels are used as drive wheel for assist control.

Because no reduction gears and no gear backlash are present in the units, the motors can drive the wheel directly.

B. Physical Model of EV

When the current control of motor is fast enough, EV mode can be shown as Fig. 2. Motion equation of wheel and vehicle body can be given as (1), (2).

$$J_{\omega_{ij}} \dot{\omega}_{ij} = T_{ij} - r F_{dij}, \quad (1)$$

$$M \dot{V} = \sum_{i,j} F_{dij} + F_h. \quad (2)$$

Here, ω , V , T , F_d , F_h , subscript i and j represent wheel angular velocity, vehicle velocity, input torque, driving force, external force from hand, front-rear (f, r) and left-right (l, r) respectively. Driving resistance is ignored for simplicity.

Slip ratio of wheels λ is defined by (3).

$$\lambda = \frac{V_{\omega} - V}{\max(V_{\omega}, V, \epsilon)}. \quad (3)$$

where ϵ is a constant used to prevent division by zero. V_{ω} means wheel speed and is defined as (4).

$$V_{\omega} = r\omega. \quad (4)$$

When the EV is accelerating, V_{ω} is larger than V and when decelerating, V_{ω} is smaller than V . In this section, we assume the accelerating case and λ is defined as (5).

$$\lambda = \frac{V_{\omega} - V}{V}. \quad (5)$$

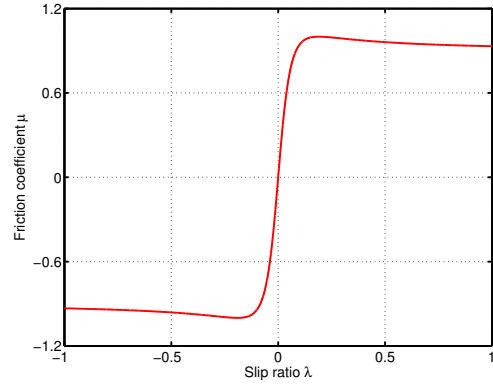


Fig. 3. Typical $\mu - \lambda$ curve.

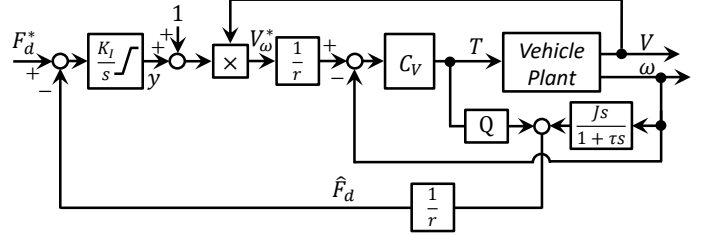


Fig. 4. Driving force control system.

Wheel driving force F_d can be calculated using friction coefficient μ and normal force N .

$$F_d = \mu N. \quad (6)$$

Typical relationship between slip ratio λ and friction coefficient μ is shown on Fig. 3. Magic formula (7) is well-known approximate expression of this relation.

$$\mu(\lambda) = D \sin(C \tan^{-1} B(1 - E)\lambda + \frac{E}{B} \tan^{-1} B\lambda), \quad (7)$$

where B, C, D and E are non-dimensional constants, usually determined according to fitting.

C. Driving Force Control

Driving force control (DFC) was proposed by our research group[2]. The block diagram of DFC is shown on Fig. 4. DFC is composed of an outer loop controlling F_d , an inner loop regulating wheel angular velocity, and reference generation part based on slip ratio.

μ reaches a maximal value at λ_{peak} and decreases when λ is larger than λ_{peak} as shown on Fig. 3. Therefore, DFC system should involve slip ratio controller so that maximum driving force can be obtained. DFC contains slip ratio reference generator based on y and prevents tires from slipping. y is defined as (8) and has the same dimension as slip ratio λ .

$$y = \frac{V_{\omega}}{V} - 1. \quad (8)$$

Incidentally, F_d can be expressed as (9) by using driving stiffness D_s and λ .

$$F_d = D_s \lambda. \quad (9)$$

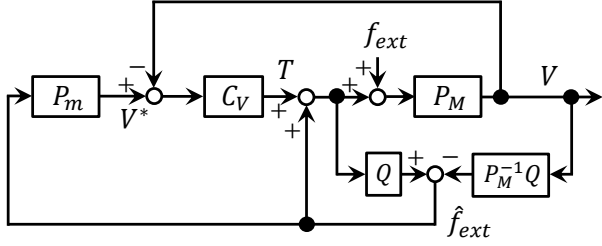


Fig. 5. Typical force sensorless impedance control system.

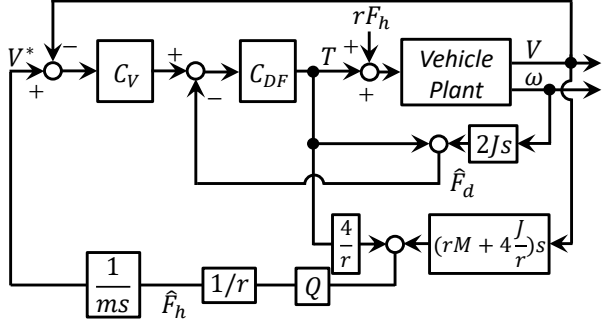


Fig. 6. Force assist control system for EV based on inertia emulation (proposed 1).

As shown on (9), λ to F_d is the zero order plant. Therefore, integrator is used for slip ratio control. By limiting the output of I controller, y falls within desired range and tire slipping can be prevented.

Driving force observer (DFO) is used to estimate forces between wheels and road F_d . DFO estimates F_d based on (10)

$$F_d = \frac{1}{r}(T - J\dot{\theta}). \quad (10)$$

D. Impedance control

Impedance control can change mechanical impedance between robot manipulation and environment such as stiffness, damping constant and mass. This control method is often used to implement assist control or impact force reduction. Fig. 5 shows the typical impedance control system based on velocity control. Velocity reference is calculated from the contact force and model impedance. Robot velocity is controlled so that the end effector emulate the model impedance. In Fig. 5, external contact forces are estimated by disturbance observer.

III. EV HAND ASSISTED CONTROL

In this section, we propose to apply impedance control to EVs. Impedance control is a method for changing contact impedance of robots and is widely used for industrial robots. However, this control has never been applied to EVs yet.

There are various applications of force control for EV that are impossible to achieve for internal combustion vehicles, such as hand assisted parking. This section discusses how to apply impedance control to EV and 3 methods are proposed.

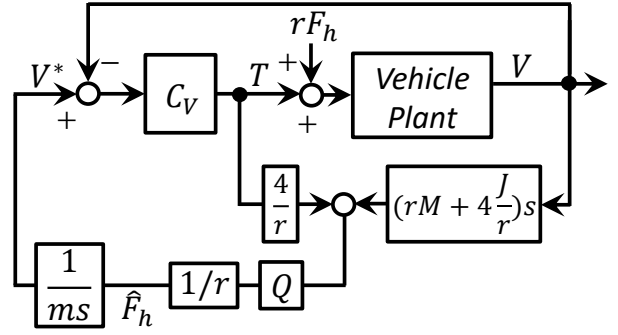


Fig. 7. Force assist control system for EV based on inertia emulation (proposed 2).

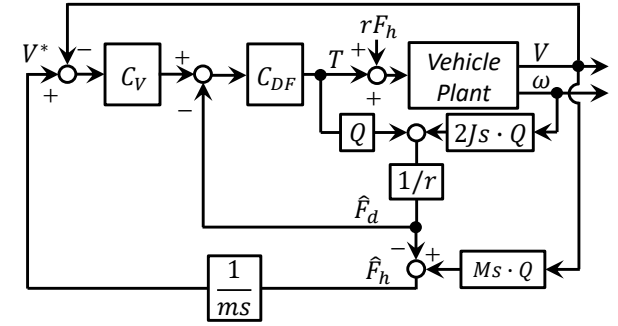


Fig. 8. Force assist control system for EV based on inertia emulation (proposed 3).

A. Simplified DFC for hand assist parking and external force estimation

Expression (2) shows that it is necessary to control driving force F_d in order to achieve inertia emulation. By controlling F_d , robustness against road surface change increases. On the other hand, the number of loops should be minimized to ensure the stability and response.

Since the velocity of EV is limited to low speed region in assist control, the wheel slip is very small. Thus, the driving force does not reach saturation point in assist control and slip ratio reference generator is not necessary. In order to increase the system stability, the reference generation part is removed from DFC for assist control.

Since F_h means external force from human hands, high response is not much important for vehicle speed control. For this reason, wheel angular velocity control is removed and a simple structure is adopted.

When λ is assumed to be zero, relationship of F_h and T is expressed as (11).

$$\hat{F}_h = (rM + 4\frac{J}{r})\dot{\omega} - \frac{4}{r}T. \quad (11)$$

Here, only the translational motion is considered and the input torque F_h can be estimated from (11). The fact that F_h contains the effect of road surface change and travel resistance should be noted.

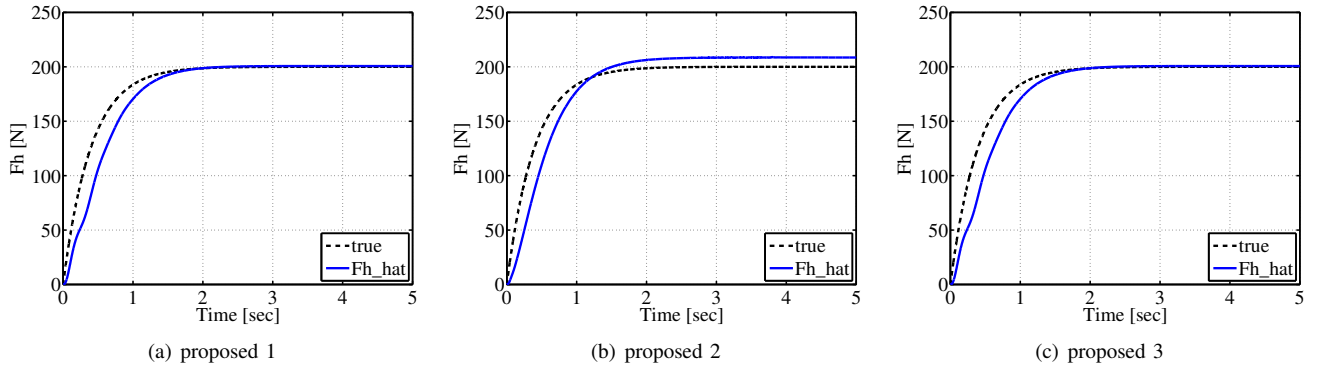


Fig. 9. Simulation result of F_h estimation.

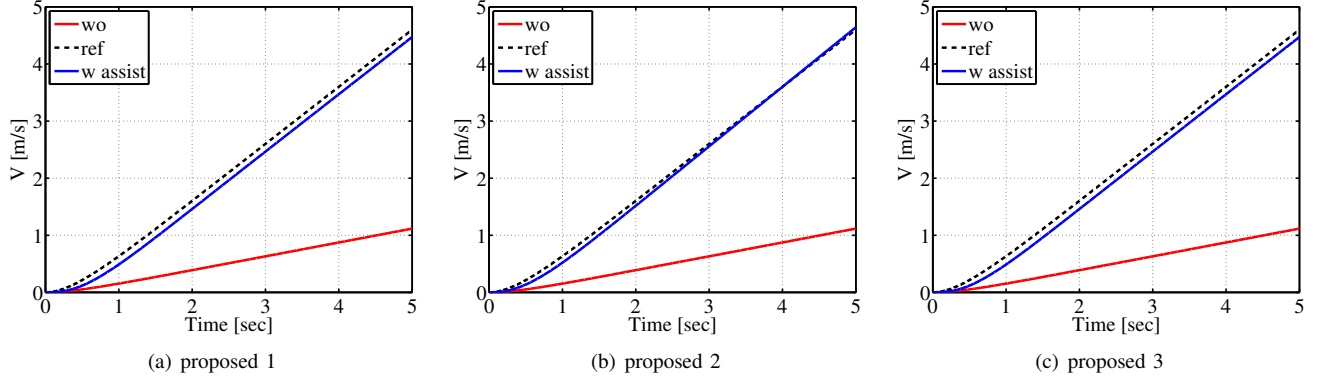


Fig. 10. Simulation result of V .

TABLE II
COMPARISON OF PROPOSED METHODS.

	style of DOB	driving force control	road surface change	quantization noise
proposed 1	1DOB	w	good	√
proposed 2	1DOB	w/o	bad	√
proposed 3	2DOB	w	very good	×

B. Proposal of impedance control for EVs

By incorporating DFC and F_h estimation, it becomes possible to apply impedance control to EV. Fig. 6 shows the block diagram of proposed assist control system (proposed method 1). Prop.1 consists of 4 parts; F_h estimation, velocity reference generation, vehicle speed control loop, and simplified DFC. By emulating smaller inertia model, assist control of EV is realized.

Resolvers are often used for wheel angular position detection and its resolution is not so high. Considering measurement accuracy, proposal 1 adopt as simple structure as possible.

C. Effect of driving force control

The necessity of driving force control is discussed in this section. Fig. 7 shows the block diagram of assist control system without DFC (proposal 2). By removing F_d and V from (1)-(5), (12) can be obtained.

$$\frac{\omega}{T} = \frac{1}{(J_w + r^2 M(1 - \lambda))s}. \quad (12)$$

Because the vehicle speed is low in this system, wheel slip can be ignored. Assuming $\lambda = 0$ in (12), (13) is obtained. This approximation comes out as a modeling error.

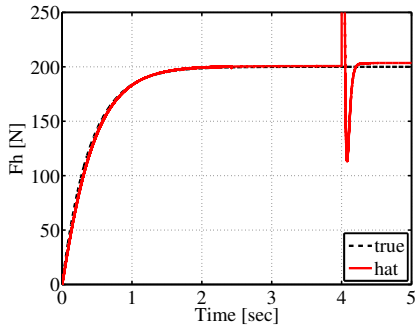
$$\frac{\omega}{T} = \frac{1}{(J_w + r^2 M)s}. \quad (13)$$

From (13), PI controller is used for wheel angular control and pole placement.

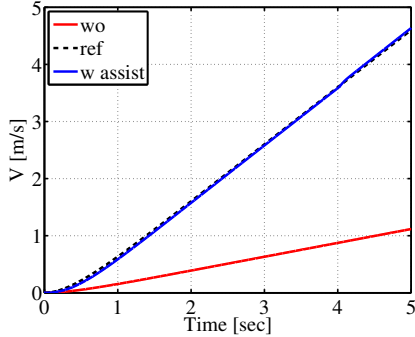
Since the proposed method 2 has fewer loops and simple structure, the system stability is improved.

D. F_h estimation method

There are 2 ways to observe F_h . One is single DOB embedded in proposal 1 and the other uses two DOB. In proposed method 1, in order to estimate external force F_h , vehicle body and wheel plant are regarded as one and the slip ratio is assumed to be 0. Single DOB method is robust to quantization noise and appropriate for wheel resolver, whose resolution is not high. However, this method cannot separate the effect of road surface change from F_h . To eliminate the

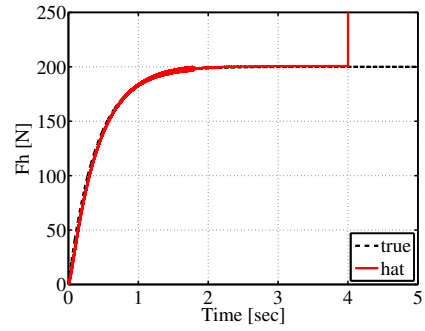


(a) Estimated external force \hat{F}_h

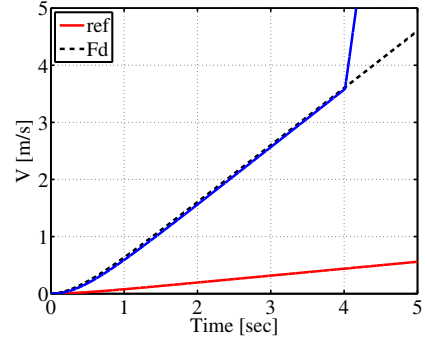


(b) Vehicle velocity

Fig. 11. Robustness against slip (proposed 1).



(a) Vehicle velocity



(b) Estimated external force \hat{F}_h

Fig. 12. Robustness against slip (proposed 2).

assumption that $\lambda = 0$, two DOB must be combined. On the following pages, this method is called proposal 3. The estimation formula of proposal 3 are the following.

$$\hat{F}_h = M\dot{V} - \hat{F}_d, \quad (14)$$

$$\hat{F}_d = J\dot{\omega} - T. \quad (15)$$

Proposed method 3, at first, estimates F_d based on input torque and wheel angular velocity. Next, external force F_h is estimated using \hat{F}_d and vehicle speed.

Fig. 8 shows the block diagram of proposed method 3.

IV. SIMULATION

This section discusses which of proposed method 1~3 is adequate by the use of numerical simulations.

A. Simulations in ideal condition

Simulation of hand assist control for EV is conducted. In the simulation, external force works on the EV plant simulating that human hand pushing vehicle body. The vehicle body is controlled as if the total mass would become 200 kg even though true mass of EV body is 854 kg.

Controllers are designed by means of pole placement. Poles of driving force controllers are placed on 10 rad/s and those of vehicle speed controllers are placed on 3 rad/s. However, because driving force is not controlled in proposed method 2, only vehicle speed poles are placed.

Fig. 9 and 10 shows the simulation result of proposed method 1~3. Fig. 9 shows the estimated F_h and Fig. 10 shows the vehicle speed. F_h is estimated correctly to some extent

in all figures. The blue and red lines of Fig. 10 mean the vehicle speed with and without control. The black line shows the velocity of imaginary vehicle whose mass is 200kg, taken as reference. From the fact that blue line overlaps the black line, intended control design is achieved.

Vehicle moves faster when assist control is added than the no assistance case, although the same force is applied. Blue line tracks to black line, meaning that the vehicle speed is controlled as if the EV mass is equal to 200 kg.

B. Effect of driving force control on road surface change

By comparing proposed 1 and 2 on simulations, necessity of DFC is discussed. In addition to former conditions, road surface change is reflected on these simulation. The friction coefficient of the road μ is reduced from 0.8 to 0.2 at 4 sec and its effect is checked.

The simulation results of proposal 1 and 2 are respectively shown on Fig. 11 and Fig. 12. Though the road surface condition have an effect on F_h estimation, proposed method 1 works well. On the other hand, in proposed method 2, F_h does not converge to true value and the assist control system diverges from reference.

C. Effect of quantization error

The wheel angular velocity is acquired by the resolver. The proposal 1 and 3 are compared by a simulation on condition that wheel angle is discretized by resolver. There is a large quantization error in the estimated F_h , leading to decreased

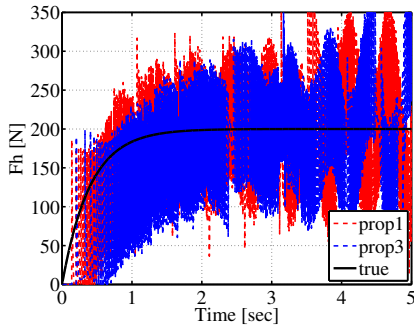


Fig. 13. Estimation method and quantization noise.

control performance. Proposal 1 and 3 are compared by simulation considering quantization error. The cutoff frequencies of proposal 1 is set to 8 rad/s, and that of proposal 3 is decided so that the noise ripple of both methods become same order. Fig. 13 shows the estimated F_h . Each black, red, blue line means true F_h , proposal 1, and 3.

In order to achieve same estimation accuracy, the cutoff frequency of proposal 3 must be set to 2 rad/s. It is 4 times lower than that of proposal 1.

V. EXPERIMENTAL RESULTS

In the experiment, proposed method 1 is considered. In the experiment, the rear wheels are used for the assist control and constant input torque equivalent to 200 N is applied, in order to emulate the F_h . Since the slip is small enough to be ignored, average of the angular velocity of rear wheels is used to calculate vehicle speed V .

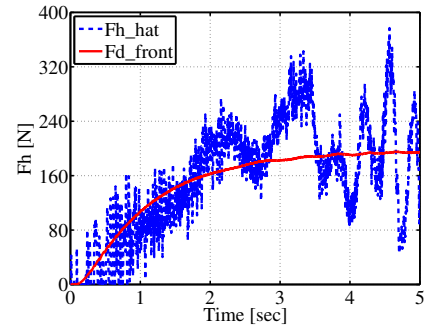
Fig. 14 shows the experimental result. The blue line in the Fig. 14(a) shows the smoothed \hat{F}_h and the red line shows the \hat{F}_d of front wheels of the case without control. Fig. 14(b) shows the vehicle speed with assist control. The experimental result is similar to Fig. 9 and thus the assist control is achieved. There's great amount of quantization noise on the estimated force which makes the velocity reference vibrating.

Vehicle acceleration in the Fig. 14(b) is slower than Fig. 10. The experimental vehicle speed at 5 sec is only 1/3 of simulation. Rolling frictions, travel resistance and starting torque, which are not considered in the simulations, are the main reasons.

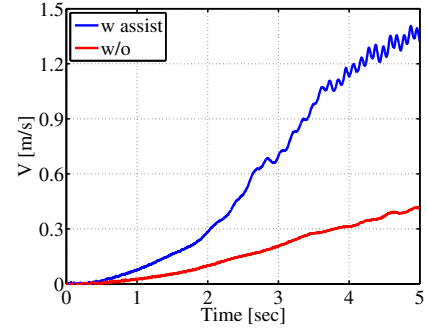
VI. CONCLUSION

In this research, force assist control for EV is proposed based on inertia emulation and its effectiveness was demonstrated by simulations and experiments. Thanks to this proposed method, back drivability of EVs can be arbitrarily chosen and EVs can be easily moved by human hand. One main application of this backdrivable EV is novel human-friendly parking method.

Further study contains lateral force estimation and external gravity force compensation.



(a) Estimated external force F_h .



(b) Vehicle velocity.

Fig. 14. Force assist control for EV (experiment).

ACKNOWLEDGMENT

This research was partly supported by Industrial Technology Research Grant Program from New Energy and Industrial Technology Development Organization (NEDO) of Japan (number 05A48701d), the Ministry of Education, Culture, Sports, Science and Technology grant (number 22246057 and 26249061).

REFERENCES

- [1] Y. Hori, "Future vehicle driven by electricity and control - Research on four-wheel-motored "UOT Electric March II", *IEEE Transactions on Industrial Electronics*, vol. 51, no. 5, pp. 954–962, 2004.
- [2] M. Yoshimura and H. Fujimoto, "Driving Torque Control Method for Electric Vehicle with In-Wheel Motors," *IEEJ Transactions on Industry Applications*, vol. 131, no. 5, pp. 721–728, 2011.
- [3] W.-P. Chiang, D. Yin, M. Omae, and H. Shimizu, "Integrated Slip-Based Torque Control of Antilock Braking System for In-Wheel Motor Electric Vehicle," *IEEJ Journal of Industry Applications*, vol. 3, no. 4, pp. 318–327, 2014.
- [4] K. Fujii and H. Fujimoto, "Traction control based on slip ratio estimation without detecting vehicle speed for electric vehicle," in *Fourth Power Conversion Conference-NAGOYA, PCC-NAGOYA 2007 - Conference Proceedings*, 2007, pp. 688–693.
- [5] T. Yoshioka, "Stable Force Control of Industrial Robot Based on Spring Ratio and Instantaneous State Observer," *IEEJ Journal of Industry Applications*, vol. 5, no. 2, pp. 132–140, 2016.
- [6] N. Motoi, "Human Machine Cooperative Grasping / Manipulating System Using Force based Compliance Controller with Force Threshold," *IEEJ Journal of Industry Applications*, vol. 5, no. 2, pp. 39–46, 2015.
- [7] H. Tsung-Hua, L. Jing-Fu, Y. Pen-Ning, L. Wang-Shuan, and H. Jia-Sing, "Development of an automatic parking system for vehicle," *Vehicle Power and Propulsion Conference, 2008. VPPC '08. IEEE*, pp. 1–6, 2008.
- [8] M. R. Dizaji, M. R. H. Yazdi, M. A. Shirzi, and Z. Gharehnozifam, "Fuzzy supervisory assisted impedance control to reduce collision impact," in *RSI/ISM International Conference on Robotics and Mechatronics, ICRoM 2014*, 2014, pp. 858–863.